

Received 18 June 2025, accepted 11 July 2025, date of publication 14 July 2025, date of current version 23 July 2025.

Digital Object Identifier 10.1109/ACCESS.2025.3589009



RESEARCH ARTICLE

Transport Capacity Maximization in Rail Mass Transit Stations Under Uncertainty

ADRIÁN FERNÁNDEZ-RODRÍGUEZ[✉], MARÍA DOMÍNGUEZ[✉], ASUNCIÓN P. CUCALA[✉],
AND ANTONIO FERNÁNDEZ-CARDADOR[✉]

Institute for Research in Technology, ICAI School of Engineering, Comillas Pontifical University, 28015 Madrid, Spain

Corresponding author: Adrián Fernández-Rodríguez (adrian.fernandez@iit.comillas.edu)

This work was supported by Project FUTURAIL (CPP2021-008372) funded by Agencia Estatal de Investigación (AEI)/the Spanish Ministerio de Ciencia, Innovación y Universidades (MICIU)/AEI/10.13039/50110001103 and by European Union NextGeneration EU/Plan de Recuperación, Transformación y Resiliencia (PRTR).

ABSTRACT Urban railways play a critical role in promoting sustainable transportation by providing high-capacity, efficient, and low-emission alternatives to road-based travel. As cities continue to grow, the demand for mass transit rail transport is steadily increasing, posing significant challenges to existing infrastructure, particularly at terminal stations, which often become bottlenecks due to their complex operations. Addressing these capacity limitations is essential not only for improving the quality of service but also for supporting the broader goals of urban sustainability. This paper introduces a two-level optimization model designed to maximize the practical transport capacity of mass transit railway stations. At the upper level, a genetic algorithm determines the optimal sequence of train services and platform assignments. These solutions are then evaluated by a linear programming model at the lower level to estimate the resulting transport capacity. For a more realistic assessment of practical capacity, fuzzy modelling is employed to manage uncertainties in train delays and operational variations. The model incorporates critical operational constraints of urban railways, including minimum turn-around times, track occupancy, and constant headways between train services of the same type. A detailed simulation model is used to evaluate route intervals based on train dynamics and signalling systems. Simulation results based on real-world data demonstrate the model's effectiveness in maximizing capacity under uncertain conditions and different operational schemes, contributing to more efficient and sustainable mass transit railway systems. This research highlights the importance of optimizing rail transport capacity as a key component of sustainable urban development.

INDEX TERMS Mass transit railway, transport capacity, fuzzy logic, genetic algorithm, bi-level optimization.

I. INTRODUCTION

Railways are recognized as a high-capacity, efficient, and safe mode of transport. These features make them essential for metropolitan mobility, attracting millions of passengers globally. Along with the growth in the population of cities, this leads to a continuous increase in demand for urban rail services. Consequently, many existing railway lines face a significant challenge of operating near or at their maximum capacity.

The associate editor coordinating the review of this manuscript and approving it for publication was Jesus Felez[✉].

One of the key performance metrics in rail systems is transport capacity, defined as the maximum number of trains that can operate per hour within a segment of the railway line. This capacity is influenced by several physical and operational factors such as the infrastructure layout [1], the performance of trains [2], or the signalling system installed [3]. In addition, how the system is operated also critically impacts the transport capacity. Thus, the traffic in the railway system must be considered when assessing the transport capacity [4].

The project FUTURAIL [5] tackles the interrelation of these factors in transport capacity. The main objective of this project is to provide an integrated model to manage transport capacity efficiently in modern highly demanded urban

and metropolitan railway lines, along with software tools to implement it. As part of the FUTURRAIL project, this paper presents the model developed to assess and maximize the transport capacity in urban rail terminal stations.

Different bottlenecks can be found in a railway line, which determines the capacity of the whole system. In particular, terminal stations are frequently critical nodes in mass transit railways in terms of transport capacity because of their complex layout and operation. For instance, incompatible routes converge in terminal stations, direct trains face reversing ones, and dwell times are higher when changing train direction. Moreover, these stations have significant passenger flows because, in many cases, they are part of transport hubs with connections to other transport modes [6]. Therefore, evaluating the terminal station node is mandatory to assess the transport capacity of a line.

The scheduling of terminal station timetables for transport capacity calculation is currently a sequential process carried out by the railway infrastructure manager. First, the assignment of train types to platforms is decided, and then the sequence of entry and exit maneuvers is designed. Then, the UIC timetable compression method is applied to calculate the associated capacity [7]. Finally, to ensure that small delays are not propagated to other trains, time margins between services must be included. These margins are usually introduced by the infrastructure manager only after the entry and exit timetable pattern has been generated [8].

With the aim of addressing this complex operation, this paper proposes a two-level optimization model that allows the calculation of the maximum practical transport capacity of a mass transit railway station, as well as the timetable and the platform assignment that maximize the capacity usage.

At the upper level of the optimization procedure, a genetic algorithm (GA) seeks the best sequence of services and platform assignment. Then, the solutions of the GA are evaluated in terms of transport capacity at the lower level using a linear programming model. As in the literature, the signalling system constraints, minimum turn-around time, occupancy time and number of tracks at stations will be taken into account. As a novelty, additional constraints are included to represent the mass transit railway operation, such as a constant headway between services of the same type and platform assignment depending on the service type. Moreover, a simulation model with a detailed representation of the train dynamics and ETCS (European Train Control System) braking curves is applied to obtain the minimum and realistic interval between the different routes and configure the optimization model.

Compared to the conventional approach typically used by railway administration managers, the proposed capacity optimization method simultaneously addresses both the assignment of service types to platforms and the sequencing of station entry and exit maneuvers. Therefore, the model is capable of finding better solutions that maximize capacity. In addition, the proposed model incorporates delay uncertainty through the use of fuzzy numbers, which allows for the

sizing of the time margins while simultaneously optimizing the entry and exit patterns and the platform assignments, rather than doing so sequentially in a later phase.

The main contributions of this transport capacity optimization model are:

- The use of the main mass transit operational constraints in the transport capacity model to evaluate realistic scenarios such as, regular timetables, uniform headways for services of the same line and platform assignment dependent on service line, are considered.
- The model allows for the evaluation of two operational schemes depending on whether rolling stock and train drivers can operate any service type.
- The model does not need a predefined train sequence. Instead, the model calculates the timetable and the platform assignment that maximizes the transport capacity.
- The uncertainty in operation is included in the model, making use of fuzzy parameters to produce a practical transport capacity evaluation.
- The application to a real case study highlighting the impact of the mass transit operational constraints and the uncertainty.

The paper is organized as follows: Section II reviews the related work. Section III describes the fuzzy maximum practical capacity model proposed detailing the key factors influencing railway station capacity. Section IV presents the problem definition. Section V details the solution method for the bi-level optimization model, including the integration of GA, linear programming, and fuzzy logic to account for operational uncertainties. Section VI explains the methodology used for determining the minimum interval between train routes, based on detailed simulations of train dynamics and signalling systems. Section VII applies the proposed model to a real-world case study, demonstrating its effectiveness in optimizing railway station capacity. Finally, Section VIII presents the main conclusions obtained in this piece of research.

II. RELATED WORK

The methods applied to calculate transport capacity can be divided into three categories: analytical methods, simulation methods and optimization methods [9].

Analytical methods use mathematical formulae to calculate capacity. They need little data to provide a result, which makes them adequate where detailed information about the railway system is unavailable. Although fast calculation, these methods are sensitive to parameter variation [8]. A well-known approach is the compression method proposed by the International Union of Railways (UIC), published in its 406 leaflet [10]. This method divides a railway system into different sections and compresses each timetable to obtain the capacity usage. The compression method was analyzed by Lindner [11] in 2011, highlighting that it can only be applied in conflict-free stations to obtain relevant results. As a result, the compression method was extended in 2013 [7]

to include the assessment of nodes such as the bifurcations or terminal stations. Different studies have since applied the compression method to calculate transport capacity in railway lines. In [12], a tool named MesoRail was used to calculate the occupancy rate in railway stations. The tool's analysis is based on the compression method used to calculate capacity. In [13], a compression-based method was also proposed for long-term planning at stations. Later, different methodologies were compared in [14] to obtain compressed timetables such as the combination-reconstruction approach, the triangular-gap problem, and the max-plus algebra method, and similar results were obtained. Another analytical approach for capacity evaluation was proposed in [15] for complex networks. This method allows for the evaluation of transport capacity and the production of strategic plans. In [16], several capacity assessment methods were compared, and a novel one was proposed and applied to a Lithuanian rail system. In [17], the Potthoff, probabilistic and Deutsche Bahn methods were compared to calculate station transport capacity. A novel space-time-speed method to improve station transport capacity has been proposed in [18]. Specifically, this paper used an analytical formulation to evaluate variations in transport capacity. In [19], an empirical method, based on a compression method, was developed to correlate timetable-based capacity utilization and performance at stations. A stochastic analytical method was proposed in [20] to produce a correct buffer time, estimating delays produced by conflicts between routes and deviations of transfer connections. In [21], a Lagrangian method is proposed to calculate the passing capacity of a station in a high speed railway system. Real-life trajectory data were used to assess capacity occupation via a critical path extension of UIC 406 in [22].

All the previous works evaluate the transport capacity based on a predefined timetable or a specific traffic pattern that operates the infrastructure (based on the train sequence or statistical distribution of trains). On the contrary, Jensen et al. [23] studied the strategic assessment of capacity consumption based on the compression method but without a timetable. The application of the previous model to mass transit systems, however, lacks of headway regularity or platform assignment restrictions. In [24], a Markov-chain-based analytical method was developed to evaluate junction capacity based on route topology and arrival rates. In [25], a method combining timed Petri nets and macroscopic diagrams was proposed to evaluate periodic network capacity. Later, the same authors extend the method in [26] to evaluate the transport capacity based on the demand. Both methods do not depend on fixed timetables and are intended for strategic and macroscopic purposes.

Simulation methods, on the other hand, use more detailed data to estimate transport capacity, but provide more accurate results. For this reason, they are more adequate for the microscopic assessment of existing exploitations than the analytical procedures above. Typically, simulation-based studies analyze predefined timetables and rely on software tools such as RailSys [27], OpenTrack [28], [29], [30] or

RTC [31], [32], [33], [34], [35]. These platforms allow for detailed modeling of train dynamics and infrastructure constraints, supporting accurate and scenario-specific capacity evaluations. In [36], Montecarlo simulation, three heuristics and branch and bound algorithms are compared in evaluating transport capacity under traffic disturbances. Montecarlo simulation is also used in [37] for calculating headways of different stopping patterns. In [38], a microscopic simulation model, the Infrastructure Representing Model for fixed equipment, is presented to evaluate transport capacity in railway stations. A mesoscopic simulation model is introduced in [39] to assess the transport capacity of stations, taking into account the random disturbances of train delays. The queuing theory was applied in [21] to model railway station operations, and simulation was applied to solve the model. In [40], a mesoscopic stochastic simulation model and an analytical model are used to evaluate transport capacity improvements by using an extended switch point area in a single-track railway line. Several algorithms were proposed in [41] for the automated creation of a mesoscopic target model of station throat based on consecutive transformations of an initial (intuitive) microscopic model. In [42], RailSys-based simulations were used to evaluate the capacity effects of ERTMS/ETCS Hybrid Level 3. The influence of level 3 and level 2 trains, the length of virtual subsections, and infrastructure configurations are analyzed as a function of real timetables.

Finally, optimization methods use mathematical programming models or nature-inspired algorithms. Optimization is typically used for capacity-related problems such as train scheduling and routing. For example, an optimum track allocation is performed in [43] to evaluate the transport capacity of a station. In [44], a simulated annealing algorithm is applied to determine the capacity of railway yards given a timetable. An integer programming model is proposed in [45] to measure the difference in transport capacity with different train types. Sameni et al. [46] developed a Data Envelope Analysis (DEA) to determine the efficiency of railway companies using the transport capacity. In [47], a multi-objective problem is presented to measure the trade-off between capacity, train types and corridors, and simulated annealing is proposed to solve the problem. A two-stage optimization method is introduced in [48] to calculate transport capacity depending on rolling stock and the infrastructure used. Guo et al. calculate in [49] the transport capacity of a high-speed railway station using a linear integer programming model considering the minimum turn-around time, the depot capacity and the entry and exit route sequence. The study presented in [50] develops a model for delay management that includes the capacity restriction of the stations in the platform assignment. An optimization model was proposed in [51] to calculate the transport capacity of high-speed railway stations, minimizing the track occupancy and finding the shortest path for the service. In [1], a two-stage optimization model is proposed to evaluate transport

capacity at stations without an initial timetable. In the upper stage, the compatible routes are determined by graph coloring modelling and in the second stage, the sequence of routes is modelled as a travelling salesman problem. However, typical operational restrictions in urban railways, such as headway regularity or platform assignment subject to service types, are not considered. A mixed integer programming model is applied in [52] to include new trains in a timetable to maximize a station's transport capacity, taking random delays into account. A "schedule and fix" algorithm is proposed in [53] to solve mixed integer programming for estimating capacity in different station layouts. This model takes into account different traffic patterns and flexible route choices. As before, the previous model does not take into account mass transit operational restrictions.

It is important to note that, in previous works, two different definitions of transport capacity are used: theoretical or practical transport capacity. On the one hand, to calculate the theoretical transport capacity, there is no need to consider uncertainty, given that it is assumed that trains do not deviate from the expected behavior. That means that theoretical transport capacity cannot be used to generate a commercial timetable because, in this case, if a single train were to be delayed, it would be transmitted to the rest of the trains in the line. As a result, the quality of service would be continuously degrading. In contrast, practical transport capacity refers to the volume of traffic that can run in the system permanently with a reasonable quality of service. This requires including time margins between services to ensure small delays are not transmitted to other trains. Consequently, practical capacity always has a lower value than theoretical capacity. Any model that aims to calculate the practical transport capacity must include the uncertainty inherent in train operations.

In order to represent those delays, many studies use stochastic models that require reliable historical data. However, delay information is unavailable when assessing new infrastructure, and it can no longer be valid in existing installations if the operation changes. In contrast, fuzzy modelling can work with imprecise or incomplete data, therefore, the representation of the uncertainty associated to time delays by means of fuzzy numbers [54] presents advantages when calculating capacity. Fuzzy modelling can work with imprecise or incomplete data. Furthermore, it is flexible and simple to implement, providing fast calculation times. Several studies on railways have already applied an uncertainty model using fuzzy numbers, proving its suitability. For example, in [55], a fuzzy optimization model is proposed for rescheduling high-speed trains. In [56], the optimal speed profiles in urban DC railways are designed, with fuzzy numbers representing the running time and energy consumption. A model is proposed in [57] to obtain a timetable in the planning stage with fuzzy passenger demand. In [58], a model to design jointly timetable and speed profiles using a fuzzy model of delays and punctuality constraints is proposed. The model presented in [45] uses fuzzy knowledge to consider the frequency of accidents and obtains the transport capacity of a railway

station using an analytical model. The algorithm proposed in [59] obtains speed profiles for urban automatically driven railways where the mass uncertainty is modelled as a fuzzy number. In [60] and [61], the uncertainty in applying manual driving commands is modelled using fuzzy knowledge. In [30], new capacity measures, fuzzy maximum capacity and fuzzy occupancy time rate, are proposed and obtained using an OpenTrack model and fuzzy dwell times.

III. FUZZY MAXIMUM PRACTICAL CAPACITY OF A STATION

This section presents the core elements of the proposed model, which is structured into two primary components: an uncertainty delay model and a practical capacity model.

A. UNCERTAINTY DELAY MODEL

The transport capacity model proposed takes into account the uncertainty in arrival and departure hours of the service because of the delays accumulated during the operation. The model aims to represent the vagueness in the knowledge regarding the delays because of the uncertainty of train operation using fuzzy numbers to represent arrival and departure times [54]. As a consequence, the transport capacity result is a fuzzy number as well.

In the proposed model, each train event i , either an arrival or a departure, has an associated time (t_i) represented as a fuzzy number \hat{t}_i . This allows for incorporating uncertainty into scheduling. Various membership functions $\mu_{\hat{t}_i}(t)$ can be employed, such as hyperbolic, exponential or piece-wise linear functions [62] or S-shaped functions [63], [64]. In this case, triangular membership function is used to model the events' hour.

The fuzzy arrival/departure time of a service is represented in Figure. 1 and by (1). The arrival/departure time with an associated possibility value of 1 (which is the core of the fuzzy number) is t_i . This is the value that will be published in the commercial timetable. On the other hand, the lower limit of the support is t' and the upper limit of the support is t'' .

$$\mu_{\hat{t}_i}(t) = \begin{cases} 0; & \text{if } t < t' \\ \frac{t - t'}{t_i - t'}; & \text{if } t' \leq t \leq t_i \\ \frac{t'' - t}{t'' - t_i}; & \text{if } t_i \leq t \leq t'' \\ 0; & \text{if } t > t'' \end{cases} \quad (1)$$

B. PRACTICAL CAPACITY MODEL

The aim of the practical capacity model is to determine the optimal traffic pattern that maximizes the practical capacity of a mass transit railway station. The model considers K different types of services, which correspond to the lines that converge at the station, and there are M platforms where trains can arrive at or depart from. The input information is the number of services of each type $\overrightarrow{N_{serv}} = \{n_1, n_2 \dots n_K\}$ that arrive and depart from the station in the time period studied.

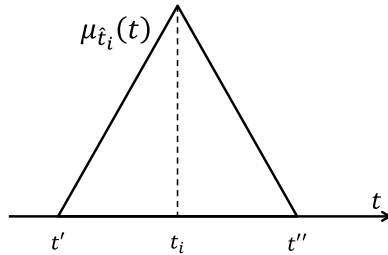


FIGURE 1. Fuzzy arrival/departure time of a service.

Thus, the total number of arrival and departure events in the timetable period is NS , that can be calculated as two times (arrivals + departures) the sum of the number of services of each type (Eq. (2)).

$$NS = 2 \cdot \sum_{k=1}^K n_k \quad (2)$$

The output of the model is the minimum time length for the period (W), the associated arrival and departure of each service \vec{T} , and the target platform for each type of service \vec{P} .

For train conservation, the number of arrivals of a service type must be equal to the number of services of each type in the time period as shown in (3). This condition is established as well for the number of departures of a service type using (4).

$$\sum_{i=1}^{NS} \delta_{i,k}^a = n_k \quad k \in [1, K] \quad (3)$$

$$\sum_{i=1}^{NS} \delta_{i,k}^d = n_k \quad k \in [1, K] \quad (4)$$

where δ_{ik}^a is a binary variable that is equal to 1 if the event i is an arrival of a service type k , and δ_{ik}^d is another binary variable that is equal to 1 if event i is a departure event of a service type k .

Moreover, an arrival at a platform must occur between two consecutive departures from the same platform for train conservation. Similarly, a departure from a platform must occur between two consecutive arrivals at the same platform to observe the platform capacity of one train stopped. This can be ensured with the restrictions modelled by (5), (6). In the case of equation (5), between any two departure events assigned to a platform, there exists at least a number of arrival events assigned to the same platform equal to the number of departure events to this platform in the interval (including the two departures in the extremes) minus 1. If the interval only contains two departure events from the platform at the extreme of the considered interval, at least one arrival event to this platform must occur between them. The same reasoning can be applied to equation (6), but changing departures for arrivals and vice versa. Both equations applied at the same time, make that feasible solutions are those where arrivals and

departures assigned to a platform are alternating. Additionally, (7) ensures that an event only represents an arrival or a departure of a specific service type.

$$\sum_{k=1}^K \sum_{t=i}^j \beta_{t,m} \delta_{t,k}^d \leq 1 + \sum_{k=1}^K \sum_{r=i+1}^{j-1} \beta_{r,m} \delta_{r,k}^a \quad i \in [1, NS-2]; j \in [i+2, NS]; m \in [1, M] \quad (5)$$

$$\sum_{k=1}^K \sum_{t=i}^j \beta_{t,m} \delta_{t,k}^a \leq 1 + \sum_{k=1}^K \sum_{r=i+1}^{j-1} \beta_{r,m} \delta_{r,k}^d \quad i \in [1, NS-2]; j \in [i+2, NS]; m \in [1, M] \quad (6)$$

$$\sum_{k=1}^K (\delta_{i,k}^a + \delta_{i,k}^d) \leq 1 \quad i \in [1, NS] \quad (7)$$

where $\beta_{t,m}$ is a binary variable that is equal to 1 if the event t will arrive at or depart from platform m .

The platforms of the station are reserved for services of the same type. That means that the departure of a service type always occurs from the same platform to help passengers find their train. In the proposed model, the terminal station topology analyzed in this study is of the “stub-end” type, where trains arrive and depart from the same platform due to the absence of the possibility to switch tracks via reverse maneuvers behind the station. Considering this topology, two different operational scenarios can be assumed for the station exploitation.

- Fixed platforms for arrivals and departures of the same service type. In this case, the rolling stock is different depending on the service type and/or the drivers assigned to the rolling stock have to operate the same line of the railway system. Consequently, it is mandatory that the trains performing a service type arrive at the platform assigned to the departures of the same service type. Thus, trains connect arrivals and departure services of the same type. To model this case, it is necessary to include equation (8).

$$\beta_{i,m} (\delta_{i,k}^d + \delta_{i,k}^a) = \beta_{j,m} (\delta_{j,k}^d + \delta_{j,k}^a) \quad i, j \in [1, NS], k \in [1, K] \quad (8)$$

- Fixed departure platforms for the same service type with flexible arrivals. In this case, the rolling stock is similar for all the service types and the drivers assigned to the rolling stock can operate in any line of the railway system. Therefore, arriving trains can be assigned to any platform independently of the service type that they are performing. Thus, trains will connect an arrival service of a type with the departure service assigned to its platform (that can be of a different type). To model this case, equation (9) is included instead of equation (8).

$$\beta_{i,m} \delta_{i,k}^d = \beta_{j,m} \delta_{j,k}^d \quad i, j \in [1, NS], k \in [1, K] \quad (9)$$

In both cases, equation (10) must be satisfied to ensure that each event is assigned to a single platform.

$$\sum_{m=1}^M \beta_{i,m} = 1 \quad i \in [1, \text{NS}] \quad (10)$$

The previous conditions need to satisfy that the number of platforms is greater than or equal to the number of service types as shown in (11).

$$M \geq K \quad (11)$$

The problem is subject to safety constraints (the minimum interval between each pair of routes) and operational requirements (regular headway between services of the same type).

It is necessary to consider the trains of the previous time period of the timetable to include the restrictions imposed by them. Therefore, the difference between the departure/arrival hours of trains and the departure/arrival hours of trains in the previous time period will be equal to the time length of the timetable period, given a traffic pattern and a platform assignment. That means that all the events in the previous time period occur exactly at the same time but are displaced one period into the past. This is modelled by the constraint represented in (12).

$$\hat{t}_i - \hat{t}p_i = \hat{W} \quad i \in [1, \text{NS}] \quad (12)$$

where \hat{t}_i is the fuzzy arrival or departure time for the arrival/departure event i , $\hat{t}p_i$ is the fuzzy hour of the same event but in the previous time period and \hat{W} is the fuzzy length of the time period.

A minimum distance between trains must be respected for safe operation. This is modelled using the minimum time interval constraints shown in Eq. (13) for services in the same time period and in Eq. (14) to compare with services in the previous time period. In train operation, the minimum distance between trains can be translated as the minimum time interval that must be observed between every two events. This minimum distance is related to the topology of the station and, therefore, the minimum interval depends on the two routes considered; i.e., the arrival/departure platform. Furthermore, the minimum interval depends on the rolling stock that runs on the routes, as different rolling stocks perform different running times. As the rolling stock is dependent on the service type, the minimum interval that restricts the closeness of two events depends on the arrival/departure platform and the rolling stock of the two events considered.

$$\begin{aligned} \hat{t}_i - \hat{t}_j \geq & \sum_{x=1}^K \sum_{y=1}^K \sum_{m=1}^M \sum_{l=1}^M [\beta_{i,m} \beta_{j,l} (\delta_{i,x}^a \delta_{j,y}^a \text{Iaa}_{x,y}^{m,l} \\ & + \delta_{i,x}^a \delta_{j,y}^d \text{Iad}_{x,y}^{m,l} + \delta_{i,x}^d \delta_{j,y}^a \text{Ida}_{x,y}^{m,l} \\ & + \delta_{i,x}^d \delta_{j,y}^d \text{Idd}_{x,y}^{m,l})] \quad i \in [1, \text{NS}]; j \in [1, i] \quad (13) \end{aligned}$$

$$\begin{aligned} \hat{t}_i - \hat{t}p_j \geq & \sum_{x=1}^K \sum_{y=1}^K \sum_{m=1}^M \sum_{l=1}^M [\beta_{x,m} \beta_{y,l} (\delta_{i,x}^a \delta_{j,y}^a \text{Iaa}_{x,y}^{m,l} \\ & + \delta_{i,x}^a \delta_{j,y}^d \text{Iad}_{x,y}^{m,l} + \delta_{i,x}^d \delta_{j,y}^a \text{Ida}_{x,y}^{m,l} \\ & + \delta_{i,x}^d \delta_{j,y}^d \text{Idd}_{x,y}^{m,l})] \quad i \in [1, \text{NS}]; j \in [1, \text{NS}] \quad (14) \end{aligned}$$

where $\text{Iaa}_{x,y}^{m,l}$ is the minimum interval between the arrival of a service of type y at platform l and the arrival of a service of type x at platform m , $\text{Iad}_{x,y}^{m,l}$ is the minimum interval between the departure of a service of type y from platform l and the arrival of a service of type x at platform m , $\text{Ida}_{x,y}^{m,l}$ is the minimum interval between the arrival of a service of type y at platform l and the departure of a service of type x from platform m , and $\text{Idd}_{x,y}^{m,l}$ is the minimum interval between the departure of a service of type y from platform l and the departure of a service of type x from platform m . The value of these minimum intervals is calculated using the procedure detailed in Section VI.

Finally, the operational requirement of constant headway between services of the same type is modelled by Eq. (15) for trains in the same period and Eq. (16) for trains in the previous period. These constraints establish that the difference between the core value of an event's fuzzy arrival or departure hours and the previous event of the same type must be equal. The core value of the fuzzy numbers has been chosen given that it is the arrival/departure time with the highest possibility value associated and, consequently, the value that will determine the published timetable.

$$\begin{aligned} t_i - t_j = & h_{s_k} (\delta_{i,k}^a \delta_{j,k}^a + \delta_{i,k}^d \delta_{j,k}^d \sum_{t=j}^i \delta_{t,k}^d - 1) \\ i \in [1, \text{NS}]; j \in [1, i]; k \in [1, K] \quad (15) \end{aligned}$$

$$\begin{aligned} t_i - \hat{t}p_j = & h_{s_k} (\delta_{i,k}^a \delta_{j,k}^a \sum_{t=j}^i \delta_{t,k}^a + \delta_{i,k}^d \delta_{j,k}^d \sum_{t=j}^i \delta_{t,k}^d - 1) \\ i \in [1, \text{NS}]; j \in [1, \text{NS}]; k \in [1, K] \quad (16) \end{aligned}$$

where h_{s_k} is the value of the headway between two arrivals or two departures of trains with the same service type.

The consideration of constant headway restrictions and minimum distance restrictions significantly reduces the feasible solution space. The reason is that while the minimum interval sets a floor on how close events can be, the uniform headway establishes a rigid structure where the arrivals/departures of the same type must be as evenly distributed as possible in the traffic pattern. On the other hand, including uniform headway criteria reduces the transport capacity result because it is possible that between two arrivals/departures of the same service type, the trains must respect not only a time related to the different minimum distance restriction but also an additional time to respect the uniform headway.

Finally, initial conditions are established to fix the hour of the first event in the traffic pattern. The core value for the first event fuzzy hour is set to 0 to obtain the relative

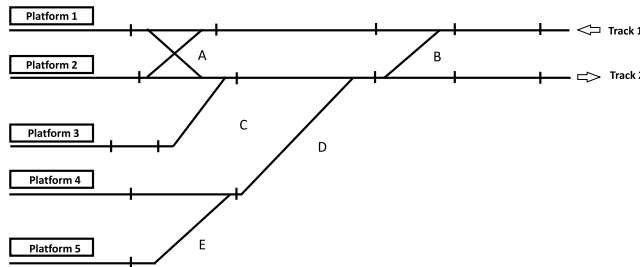


FIGURE 2. Station layout with 5 platforms.

departure/arrival hour of the other events, as shown in Eq. (17).

$$t_1 = 0 \quad (17)$$

IV. PROBLEM DEFINITION

The model proposed in this paper aims to calculate a mass transit railway station's maximum practical transport capacity. The offer of services in mass transit railways is generally based on periodical timetables where the services of each line that converges at the station run with homogeneous headways. Furthermore, trains of the same line always stop at the same station platform to be predictable for passengers.

The central objective is to identify the optimal traffic pattern, the repeated sequence of train routes during each timetable cycle, that yields the maximum practical capacity. In each traffic pattern, K types of arrival services and K types of departure services correspond to K lines that converge at the station. Two services are of the same type if both have the same origin and destination. Each of these services will have an assigned arrival/departure platform from the M platforms of the station. Consequently $2 \cdot K$ routes will be assigned to the services (M arrival routes and M departure routes). Figure 2 depicts an example of a mass transit railway station layout with 5 platforms.

The input information is the number of services from each type of service that depart/arrive at the station $\overrightarrow{N_{serv}} = \{n_1, n_2, \dots, n_K\}$ in a repetitive period of the timetable. The input $\overrightarrow{N_{serv}}$ defines the relative frequency of each type of service.

$$NS = 2 \cdot \sum_{k=1}^K n_k \quad (18)$$

With this information and the minimum interval between routes (calculated with the procedure explained in Section VI), the result will be each service's relative arrival and departure hours that minimize the length of time that the timetable period lasts. In other words, that maximizes the station's practical transport capacity.

This paper proposes a bi-level optimization model to address the problem. The objective of the upper level is to find the most adequate traffic pattern, i.e., the most adequate order of arrival/departure routes. On the other hand, the traffic pattern is evaluated at the lower level, which obtains the

minimum time window to perform all the routes, respecting the minimum time interval between each pair of routes.

V. SOLUTION METHOD

A two-level optimization procedure is proposed to solve the problem stated in Section III-B. At the upper level, the proposed genetic algorithm with fuzzy parameters seeks the best traffic pattern and platform assignment that can perform the minimum time length for the period (\widehat{W}) in the timetable. The genetic algorithm evaluates the solutions by an optimization performed at the lower level that obtains the minimum length of the period in the timetable for each solution.

The chromosome of the genetic algorithm individuals is coded using on one hand the vector for traffic pattern $\overrightarrow{S} = \{s_1, s_2, \dots, s_{NS}\}$ where each component determines, for each event, the type of service and if it is arrival or departure using an integer value. On the other hand, the genome of the genetic algorithm contains another vector, for the platform assignment, $\overrightarrow{P} = \{p_1, p_2, \dots, p_{NS}\}$ that determines for each event, the arrival/departure platform. This chromosome must satisfy constraints defined in (3), (4), (5), (6), (7) and (10). Depending on the operational case, the constraint defined by Eq. (8) or by Eq. (9) is included. The flowchart of the genetic algorithm proposed is depicted in Figure 3.

The first step in the algorithm execution is the initialization that randomly generates the initial population. Thus, NP individuals are generated. For each individual, a vector \overrightarrow{S} is generated iteratively. First of all, n_k components of vector \overrightarrow{S} are selected to be assigned to service type k . Then, randomly is decided if the first event in \overrightarrow{S} of type k is an arrival or a departure. Finally, the rest of the events of type k are assigned to be alternatively departure or arrival. Once \overrightarrow{S} is generated, \overrightarrow{P} is randomly generated to assign a platform to each service k . Using this method, the individuals obtained are feasible.

After initializing the population, each individual is evaluated to determine its fitness. The fitness of each solution corresponds to the minimum duration of the timetable period, which serves as the measure of transport capacity for the station. The evaluation function is performed by the lower level of optimization. At this level, the input variables are the traffic pattern and the platform assignment of a solution. The objective function of the lower level is the minimization of the core value of the length of the timetable period (W). The core value is used because the most possible value will be the one published in the timetable.

This objective function is subject to the constraints defined in (12), (13), (14), (15), (16) and (17) to take into account the safety distance between trains, the constant headway between services of the same type and the initial time for the first event in the period. The problem described is a linear programming problem that can be easily solved using commercial solvers such as CPLEX, GUROBI, or the function "linprog" included in MATLAB's optimization toolbox.

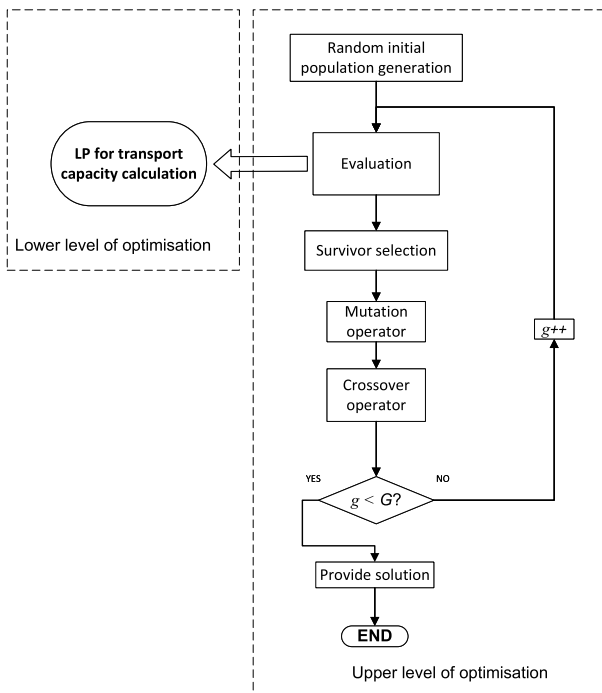


FIGURE 3. Flowchart of the genetic algorithm for capacity calculation.

Then, a binary tournament is performed to select the NE survivors for the next generation. Thus, the fittest individuals are retained in the population of the next generation.

Finally, mutation and crossover operators are performed to generate the offspring and complete the NP individuals in the next generation population:

- NM individuals are generated using the mutation operator proposed in this paper: An individual is selected from the survivors of the previous generation to be a parent for the new individual. Then, it is randomly selected if the modifications will be performed in \vec{S} or \vec{P} . If \vec{P} is selected, the arrival platform of two randomly selected types of services is swapped. Otherwise, if \vec{S} is selected, the order of two randomly selected events is swapped. In contrast with the situation where \vec{P} is modified, the modification of \vec{S} requires the reconstruction of the solution to fulfil the constraints defined in Eq. (5) and (6) (the arrival of a service of a type must occur between two consecutive departures and vice versa). The reconstruction is performed for the two service types implicated in the mutation. For each one, for an event of the service type, it is compared if the immediate event of the same service type in \vec{S} is of the same nature (arrival or departure). If it is, the event is changed to make it different to the previous, ensuring the fulfillment of (5) and (6).
- NC individuals are generated using the crossover operator proposed in this paper: Two individuals are randomly selected from the survivors of the previous generation to be the parents for a new individual. Then, the new

individual will preserve the traffic pattern \vec{S} of a parent and the platform assignment \vec{P} of the other one.

Once an offspring population is obtained, the process is repeated from the evaluation during a number G of generations.

A. CONSTRAINT HANDLING METHOD

Some traffic patterns can be unfeasible because they cannot satisfy the minimum distance constraints (equations (13) and (14)) and the constant headway between services of the same type (equations (15) and (16)). For that reason, a constraint handling method is introduced to guide the population evolution to feasible solutions.

This method consists of including a penalty factor in the fitness function for the non-compliance with the constraints [65]. This penalty factor ensures that, when comparing two infeasible solutions, the one with better fitness is closer to feasibility.

The constraint handling method applied affects the lower level, including a positive slack variable (ε_j^i and εp_j^i) in the constraints for constant headway between trains with the same service type. Thus, (15) and (16) are substituted in the LP for transport capacity calculation by equations (19) and (20).

$$t_i - t_j = h_{s_k} \cdot (\delta_{i,k}^a \delta_{j,k}^a \cdot \sum_{t=j}^i \delta_{t,k}^a + \delta_{i,k}^d \delta_{j,k}^d \cdot \sum_{t=j}^i \delta_{t,k}^d - 1) + \varepsilon_j^i \quad (19)$$

$$t_i - tp_j = h_{s_k} \cdot (\delta_{i,k}^a \delta_{j,k}^a \cdot \sum_{t=j}^i \delta_{t,k}^a + \delta_{i,k}^d \delta_{j,k}^d \cdot \sum_{t=j}^i \delta_{t,k}^d - 1) + \varepsilon p_j^i \quad (20)$$

Moreover, the objective of the lower level is modified to minimize, not only the length of the timetable period, but also the value of the slack variable (equation (21)). The value of the slack variable is multiplied by a weight (b) sufficiently big to ensure that the slack value is the minimum possible and to ensure that a feasible solution will always present a lower value of the objective function than an unfeasible one.

$$\min \left(W + b \cdot \sum_{i,j} [\varepsilon_j^i + \varepsilon p_j^i] \right) \quad (21)$$

Thus, the fitness function of the upper level will be calculated by Eq. (21) as well. This way, in the binary tournament, when comparing two feasible solutions, the solution with the lowest length of the timetable period will be selected, and the feasible solution will be selected when comparing a feasible solution with an unfeasible one.

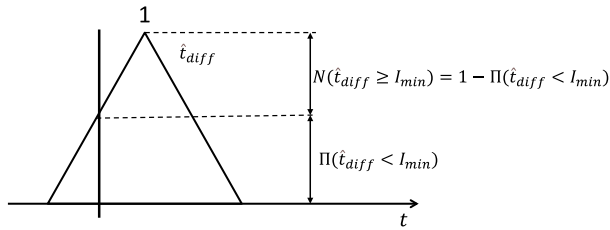


FIGURE 4. Necessity measure of minimum interval restriction fulfilment.

B. RESOLUTION OF FUZZY CONDITIONS

The resolution of the bi-level optimization problem is subject to conditions that are dependent on fuzzy numbers. First of all, there is a safety requirement that establishes a minimum time interval between two arrival/departure events in the timetable, which is imposed by the signalling system.

This requirement is defined by (13) and (14) and involves two variables defined by fuzzy numbers. These equations establish that the difference of two fuzzy times must be greater than a minimum interval. The minimum interval is the minimum time that must separate two arrival/departure events so that the preceding one does not interfere with the speed profile of the follower train. As the arrival and departure events are defined as fuzzy numbers, a robustness degree of the timetable versus delays must be defined. This is defined by (22).

$$\hat{t}_{diff} \geq I_{min} \quad (22)$$

where \hat{t}_{diff} is the difference between two arrival/departure events ($\hat{t}_{diff} = \hat{t}_i - \hat{t}_j$) and I_{min} is the minimum interval imposed by the signalling system related to these two events.

The minimum interval fuzzy constraint is illustrated in Figure 4. A required degree of time separation between trains can be defined as the necessity measure [66]. The necessity measure of observing the minimum interval I_{min} ($N(\hat{t}_{diff} \geq I_{min})$) is defined as 1 minus the possibility of violating the minimum interval in the planned operation ($\Pi(\hat{t}_{diff} < I_{min})$). If two train movements are planned with a separation that violates the minimum interval, this will result in delays in the operations as the trains cannot run closer than the distance related to the minimum interval imposed by the signalling system.

The previous condition can be solved by means of the α -cuts arithmetic [67]. As shown in Figure 4, the lower limit of the α -cut for the fuzzy time difference between two events is needed to evaluate the minimum interval restriction. The lower limit of the difference between two fuzzy numbers can be obtained as shown in Figure 5. The value of \hat{t}_{diff} decreases when the value of the time for the second event \hat{t}_i decreases. On the other hand, the value of \hat{t}_{diff} decreases when the value of the second event time \hat{t}_j increases. Therefore, the lower limit of the α -cut for \hat{t}_{diff} (t_{diff}^α) can be calculated as shown in (23).

$$t_{diff}^\alpha = t_i^\alpha - t_j^\alpha \quad (23)$$

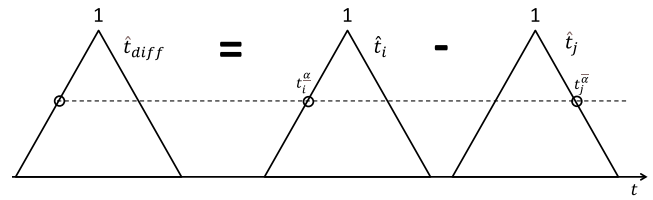


FIGURE 5. α -cuts of two arrival/departure events and the difference between them.

where t_i^α is the lower limit of the α -cut of \hat{t}_i and t_j^α is the upper limit of the α -cut of \hat{t}_j .

Finally, the restrictions for the minimum interval represented by Eq. (13) and Eq. (14) can be expressed in terms of α -cuts using Eq. (24) and Eq. (25).

$$\begin{aligned} t_i^\alpha - t_j^\alpha &\geq \sum_{x=1}^K \sum_{y=1}^K \sum_{m=1}^M \sum_{l=1}^M [\beta_{x,m} \beta_{y,l} (\delta_{i,x}^a \delta_{j,y}^a Iaa_{x,y}^{m,l} \\ &\quad + \delta_{i,x}^a \delta_{j,y}^d Iad_{x,y}^{m,l} + \delta_{i,x}^d \delta_{j,y}^a Ida_{x,y}^{m,l} + \delta_{i,x}^d \delta_{j,y}^d Idd_{x,y}^{m,l})] \\ &\quad i \in [1, NS]; j \in [1, i] \end{aligned} \quad (24)$$

$$\begin{aligned} t_i^\alpha - t_j^\alpha &\geq \sum_{x=1}^K \sum_{y=1}^K \sum_{m=1}^M \sum_{l=1}^M [\beta_{x,m} \beta_{y,l} (\delta_{i,x}^a \delta_{j,y}^a Iaa_{x,y}^{m,l} \\ &\quad + \delta_{i,x}^a \delta_{j,y}^d Iad_{x,y}^{m,l} + \delta_{i,x}^d \delta_{j,y}^a Ida_{x,y}^{m,l} + \delta_{i,x}^d \delta_{j,y}^d Idd_{x,y}^{m,l})] \\ &\quad i \in [1, NS]; j \in [1, NS] \end{aligned} \quad (25)$$

The calculation of the time period (W) also involves the difference between two fuzzy numbers, as shown in (12). Similarly, the operation restriction for a constant value of headway between two arrival events or two departure events for the same service type involves the difference between two fuzzy time events as well as can be seen in Eq. (19) and Eq. (20). However, in this case, these values are related with the timetable published for passengers. Therefore, these restrictions apply to the arrival/departure times with the highest possibility values of the fuzzy numbers. For this reason, these restrictions are written in terms of the core value of the fuzzy numbers.

VI. MINIMUM INTERVAL CALCULATION BETWEEN ROUTES

This section describes how the minimum time intervals between train movements are determined. These intervals are a critical input for the practical capacity model as they configure the minimum distance constraints (equations (13) and (14)).

The minimum interval calculation is performed through detailed simulation [68], including the ATP (Automatic Train Protection) algorithms of ETCS [69] (considering automatic train operation configuration), and applying the compression method [7]. In this simulation, the train movement and the track circuit occupation are calculated at constant time steps.

Furthermore, during the simulation, a limit brake curve model is applied to calculate the track distance that must

not be occupied in front of the train to prevent triggering an ATP braking command. That means that if the track between the train head and the limit brake curve model result is not occupied (not by a train or an assigned route), the train can circulate without interference. With this purpose, the model calculates the braking curves considering that it is circulating within the allowed limits. Then, it derives the distance between the train head and the position where the braking curves achieve a speed equal to 0 (this is the point where the end of authority must be located to not interfere with the train movement in the instant of calculation). In Figure 7, the previously described situation is depicted.

Once the simulation is performed, the compression method is applied to obtain the minimum time interval between each pair of conflicting routes at the station.

A. TRAIN MOTION MODEL

The simulation model calculates the train's position $s(t)$, speed $v(t)$ and acceleration $a(t)$ at each time step. This is achieved applying the motion equations (26), (27) and (28).

$$\frac{ds}{dt} = v(t) \quad (26)$$

$$\frac{dv}{dt} = a(t) \quad (27)$$

$$a(t) = \frac{F_m(t) + F_b(t) - (F_r(v) + F_g(s))}{\rho \cdot m} \quad (28)$$

where m is the train mass, ρ represents the effect of rotating mass, $F_r(v)$ is the running resistance and $F_g(s)$ is the resistance due to the grades and the bends (modelled as equivalent grades), $F_m(t)$ is the electrical tractive or braking effort provided by the motors, and $F_b(t)$ is the effort of pneumatic brakes. Tractive/braking effort and pneumatic braking effort depend on the train's speed and position, driving inputs, speed limits, and the train's overall length.

The initial and boundary conditions for $s(t)$ and $v(t)$ are outlined in (29) and (30).

$$s(0) = s_0, \quad v(0) = 0 \quad (29)$$

$$s(RT) = s_{end}, \quad v(RT) = 0 \quad (30)$$

where s_0 and s_{end} are the train initial and final train position, and RT is the running time of the trip between s_0 and s_{end} .

The electrical traction force $F_m(t)$ adheres to maximum and minimum limits modelled by speed-dependent curves, as illustrated in Figure 6. Pneumatic braking effort $F_b(t)$ is null when the motors are accelerating and lower than or equal to zero when braking (Eq. (31) and (32)).

$$F_{min}(v) \leq F_m(t) \leq F_{max}(v) \quad (31)$$

$$F_b(t) \leq 0 \quad (32)$$

$$F_b(t) = 0 \quad \text{if } F_m(t) \geq 0 \quad (33)$$

where $F_{max}(v)$ and $F_{min}(v)$ are the limits for electric traction and electric braking effort as a function of the train speed (v). The total braking effort combines electrical and pneumatic braking (blended braking), where pneumatic force

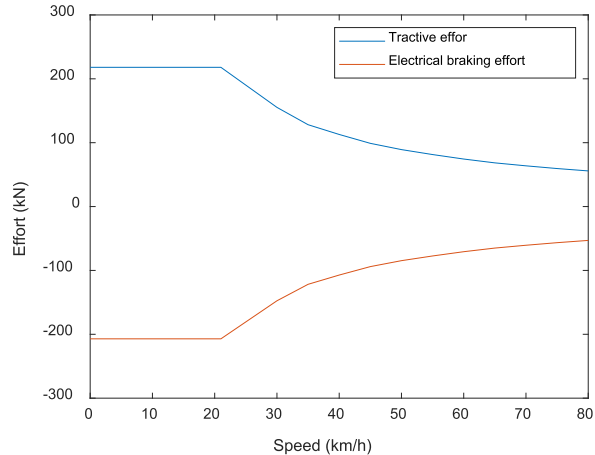


FIGURE 6. Maximum Electrical Traction/Braking curves of the train motor.

supplements the electrical braking when needed to meet deceleration requirements.

Running resistance ($F_r(v)$) is computed using the Davis equation (equation (34)) while the resistance due to grades and bends ($F_g(s)$) is calculated using (35).

$$F_r(v) = A + B \cdot v + C \cdot v^2 \quad (34)$$

$$F_g(s) = g \cdot m \cdot p(s) \quad (35)$$

where A , B and C are positive coefficients that define the running resistance, g is the gravity acceleration and $p(s)$ is the average equivalent grade in the train's position. The average equivalent gradient integrates both the mean gradient affecting the train's full length and the equivalent gradient from curve resistance. The mean gradient value includes the continuous variation of gradients and curvature along transition curves.

B. LIMIT BRAKE CURVE

A limit brake curve model is applied in the simulations to calculate the closest movement authority from a train's head not to be interfered by the ATP system (signalling system).

The limit brake curve reproduces the braking curve calculations defined in the gamma model presented in Baseline 3.6 ERTMS system requirements specifications [69].

The model is composed of several braking curves that are continuously supervised:

- Permitted Speed (P): This is the target speed that the train should not surpass. Therefore, to calculate the maximum capacity and the minimum end of authority to not interfere with the train movement, it is assumed that the train's speed and position align with the Permitted Speed curve.
- Service Brake Intervention (SBI2): This is the curve where the service brake must be initiated, considering the possible delays. This curve can be calculated from the P Curve, adding a distance obtained from multiplying the speed of the curve by a delay whose value is defined by the configuration parameter T_{driver} .

- Emergency Brake Intervention (EBI): This is the curve where the emergency brake must be initiated, taking into account the possible delays. This curve can be calculated from the SBI Curve position, adding a distance obtained from multiplying the actual train speed by a delay parameter T_{bs2} .
- Emergency Brake Deceleration (EBD): This braking curve is calculated using the safe emergency deceleration command. At this curve, the emergency brake is applied to stop the train completely. A point in EBD can be calculated from the corresponding point in EBI, taking into account the following aspects:

- V_{delta0} is added to the speed of the point in EBI to account for the inaccuracy in speed measurements.
- V_{delta1} is also added to the speed of the point in EBI to consider the period of time between the command of emergency braking and the effective traction cut-off ($T_{traction}$) where the train is maintaining its current acceleration if it is positive or null acceleration if it is negative (A_{est1}).
- V_{delta2} is also added to the speed of the point in EBI considering the period of time (T_{berem}) between the traction cut-off and the emergency brake application time ($T_{berem} = T_{be} - T_{traction}$) where the train is coasting with an acceleration A_{est2} . This acceleration is the current train acceleration but limited by a lower limit of 0 m/s² and an upper limit of 0.4 m/s².
- D_{bec} is added to the position of the point in EBI to account for the distance run in the period between the command of the emergency brake and the actual application of this command. D_{bec} is derived as the distance run by the train to achieve V_{delta1} from the current speed and V_{delta2} from V_{delta1} .

Therefore, the closest position of the end of authority to not interfere in the train movement (the limit of the braking curves) is obtained from this model by applying the following steps.

- It is considered that the train speed and position are exactly a point in the Permitted Speed curve.
- The position of the corresponding point in the EBI curve is calculated applying the different time delays configured ($v \cdot [T_{driver} + T_{bs2}]$).
- The position and speed of the point in EBD corresponding to the previously calculated EBI point are derived from the different traction cut-off and coasting period accelerations and speed inaccuracies.
- The position of the EBD curve end (where it achieves speed equal to 0) is calculated by means of the uniformly accelerated movement equations, following the configured emergency deceleration values corrected by the gradients according to system requirements specifications [69].

The previous braking curve model is devoted to manual driving operation and, for this reason, many safety margins are included. However, when talking about automatic train

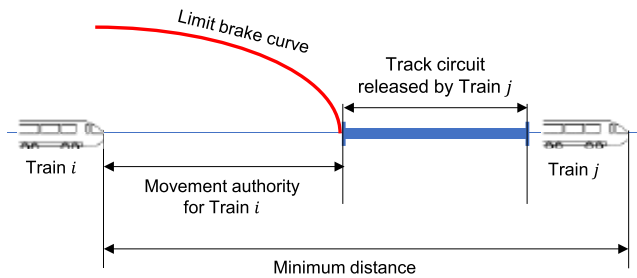


FIGURE 7. Two trains running in the same direction at the minimum distance.

operation (ATO), many of them can be ignored given the quick response and accuracy of the electronics. In particular, the following time delays has been set to 0 as it has been proposed in ATO over ERTMS working group: T_{driver} and T_{bs2} .

The result of the previous consideration is that the Permitted Speed Curve coincides with the EBI curve. Furthermore, it is similar to the typical ATP braking curves of urban railways applied in proprietary systems of the major signalling companies.

C. COMPRESSION METHOD

The compression method [7] allows to calculate the minimum time interval that must be observed between two trains so the preceding one does not interfere the speed profile of the follower train. The method proposed to calculate the minimum interval compares each pair of routes to determine conflicting points. In this method, three different scenarios can be observed:

- 1) Two routes with the same direction
- 2) Two routes with opposite directions
- 3) Arrival and departure route for the same train

In the first scenario, as the two routes run in the same direction, it is necessary to determine the piece of the track that is shared by both. Then, for each track circuit in the shared track, a minimum interval is calculated. The minimum interval is calculated assuming that the minimum safe distance between trains at one track circuit is achieved with the preceding train in the position where the track circuit is just released and the follower train is in the position where its limit brake curve is at the beginning of the track circuit. In Figure 7, an example of the positions of two trains running at the minimum distance when they have routes in the same direction is depicted.

Taking into account that these train positions are achieved at the same time, the minimum interval is calculated as shown in (36) if both trains are arriving trains, and in Eq. (37) if both trains are departing trains.

$$Iaa_{i,j} = talimit_i - tar_j \quad (36)$$

where $talimit_i$ is the running time required by train i to move from the position where the limit brake curve is at the beginning of the track circuit up to the arrival and tar_j is the

running time required by train j to move from the release of the track circuit up to the arrival.

$$Idd_{i,j} = tr_j - tlimit_i \quad (37)$$

where tr_j is the running time required by train j to release the track circuit from its departure and $tlimit_i$ is the running time required by train i to achieve the position where the limit brake curve is at the beginning of the track circuit analyzed.

Previous intervals must be modified in the case of track circuits where routes converge or diverge. In these cases, it is necessary to add to the previous time interval the time to unlock the first route, move the switch and lock the new route (t_{route}).

In the second scenario, the same procedure is applied to conflicting track circuits. In this case, the minimum interval is calculated using Eq. (38) for an arriving train followed by a departing train or Eq. (39) for a departing train followed by an arriving train.

$$Ida_{i,j} = -tlimit_i - tar_j + t_{route} \quad (38)$$

$$Iad_{i,j} = talimit_i + tr_j + t_{route} \quad (39)$$

Finally, in scenario 3, the minimum interval between an arriving service and a departing service performed by the same train is the minimum time to load and unload passengers, including the reverse maneuver.

VII. CASE STUDY

To evaluate the effectiveness of the proposed model, a case study was conducted using operational data from a real Spanish mass transit terminal station. This section describes the setup, application, and outcomes of the model under realistic conditions.

A. DATA PREPARATION

The station under analysis features $M = 5$ platforms and $K = 5$ different services that arrive at and depart from this station. In the repetitive period of the timetable, the number of arrivals of each service type is defined by vector $\vec{N} = \{3, 3, 2, 1, 1\}$. Thus, in each period $NS = 20$ arrival or departure events occur in the station. The topology of the station and the track circuit division is depicted in Figure 2. A train that enters the station zone runs approximately 250 m, and the track can be considered flat.

The rolling stock devoted to provide all the services with origin/destination at this station has the same characteristics. The mass of trains is 140 Tn, the rotative inertia coefficient (ρ) is 1.05, and the trains' length is 80 m. The maximum power of the trains motors is 3000 kW and the maximum traction effort is 250 kN. Trains' acceleration and deceleration are limited to 1 m/s^2 and 0.7 m/s^2 , respectively.

In Figure 8 and Figure 9, the possible arrival and departure routes are depicted. Most of the routes are conflicting in the track circuits that protect the bifurcations' switches. These are critical points because, apart from releasing the track circuit, it is necessary to wait the necessary time to unlock a route,

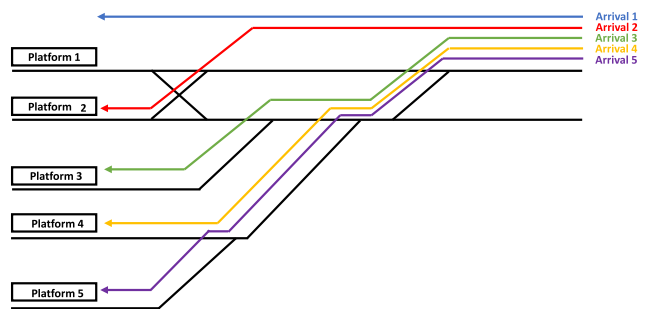


FIGURE 8. Possible arrival routes.

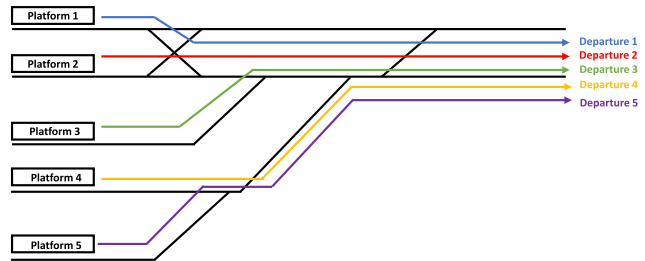


FIGURE 9. Possible departure routes.

move the switch, and lock the new route (t_{route}). Two trains with the same route are considered compatible, although they have to respect a tracking distance. However, this distance will always be observed because the second train will have a greater incompatibility with the corresponding departure route of the first train. On the other hand, a departure route will have to observe a minimum time interval with the corresponding arrival route corresponding to the minimum turn-around time. The main incompatibilities between each pair of routes are represented by Table 1. In this table, the incompatibility is referred to the bifurcations represented by lettersFigure 9, the compatible routes are represented by a dash, and the rows represent the event that occurs before the event represented by the columns.

On the other hand, two different operational scenarios are evaluated according to the information provided in Section III-B: operation with fixed platforms for arrivals and departures of the same service type, and operation with fixed platforms for departures of the same service type and flexible arrivals.

B. APPLICATION OF THE COMPRESSION METHOD

The first step to calculate the maximum practical capacity is the calculation of the minimum time interval between each pair of arrival or departure events. This information is crucial to know how close each pair of trains can run in the station.

The process explained in Section VI is applied to the case study. A minimum turn-around time (T_{turn}) of 60 s is assumed for trains that perform services 1, 2 and 3, and 45 s for trains that perform services 4 and 5. The value of the parameter t_{route} is set to 8 s to incorporate the time to unlock a previous route, switch movement and new route lock.

TABLE 1. Incompatibilities between each pair of routes. Row represents the event that occurs before the event represented by the column.

	Arrival 1	Arrival 2	Arrival 3	Arrival 4	Arrival 5	Departure 1	Departure 2	Departure 3	Departure 4	Departure 5
Arrival 1	-	A	B	B	B	T/A*	-	-	-	-
Arrival 2	A	-	B	B	B	A	T/A*	C	-	-
Arrival 3	B	B	-	D	D	B, C	B, C	T/A*	B, D	B, D
Arrival 4	B	B	D	-	E	B, D	B, D	B, C	T/A*	B, E
Arrival 5	B	B	D	E	-	B, D	B, D	B, D	B, E	T/A*
Departure 1	A	A	B, C	B, D	B, D	-	A	C	D	D
Departure 2	-	A	B, C	B, D	B, D	A	-	C	D	D
Departure 3	-	B	B	B, C	B, D	C	C	-	D	D
Departure 4	-	-	B, D	B	B, E	D	D	D	-	E
Departure 5	-	-	B, D	B, E	B	D	D	D	E	-

*The incompatibility between the departure from and arrival at the same platform is represented by a turn-around minimum time

TABLE 2. Minimum time interval between two events.

	Arrival 1	Arrival 2	Arrival 3	Arrival 4	Arrival 5	Departure 1	Departure 2	Departure 3	Departure 4	Departure 5
Arrival 1	-	51.71	51.46	50.46	50.21	T_{turn}	-	-	-	-
Arrival 2	42.21	-	44.96	43.96	43.71	8	T_{turn}	8	-	-
Arrival 3	42.46	45.46	-	44.21	43.96	8	8	T_{turn}	8	8
Arrival 4	43.46	46.46	46.21	-	44.96	8	8	8	T_{turn}	53.00
Arrival 5	43.71	46.71	46.46	45.46	-	8	8	8	53.00	T_{turn}
Departure 1	96.96	121.96	121.71	120.71	120.46	-	55.25	55.25	62.50	62.50
Departure 2	-	118.96	118.71	117.71	117.46	49.25	-	49.25	59.50	59.50
Departure 3	-	117.21	116.96	115.96	115.71	47.50	47.50	-	57.75	57.75
Departure 4	-	-	118.71	117.71	117.46	59.50	59.50	59.50	-	49.25
Departure 5	-	-	121.21	120.21	119.96	62.00	62.00	62.00	51.75	-

The train movement corresponding to every route is simulated, including the evolution of the limit brake curve. For the simulation track and train data previously presented is used. Moreover, the parameters applied for the limit brake calculation include a null value for T_{driver} and T_{bs2} , a traction cut-off time ($T_{traction}$) equals to 2 s, and an emergency brake time application of 2.5 s. After that, the compression method presented in Section VI-C is applied to obtain the minimum time distance between each pair of events presented in Table 2. In this table, the rows represent the events that occur before the events in the columns.

As can be seen, the most restrictive time intervals occur between departures and arrivals because they account for the first train travel time between its departure up to the release of the conflict track circuit, plus the second train travel time from the minimum safe distance to the critical track circuit up to its arrival. On the contrary, the least restrictive time intervals occur between arrivals and departures. In this case, many time intervals are set to t_{route} (8 s) to represent that a departure route cannot be set before all the conflicting arrival routes are finished.

C. STATION PRACTICAL CAPACITY EVALUATION FOR FIXED PLATFORMS FOR ARRIVALS AND DEPARTURES OF THE SAME SERVICE TYPE

The model presented in Section III is applied to the case study to obtain the maximum practical capacity of the station.

The arrival and departure times are fuzzy numbers with a triangular membership function as represented by (1) and Figure. 1. Each time has a core value t_i equal to the time planned for the arrival or the departure. The lower limit of the support (t') is set for all the services as t_i minus 1s. The upper limit of the support (t'') is set depending on the service type. Thus, most frequent services (services of type 1 and 2) have t'' equal to t_i plus 120s, less frequent services (services of type 4 and 5) have t'' equal to t_i plus 45s, and service of type 3 has t'' equal to t_i plus 90s. A necessity measure of observing the minimum interval is established as $N(\hat{t}_{diff} \geq I_{min}) = 0.5$ to provide robustness to the timetable.

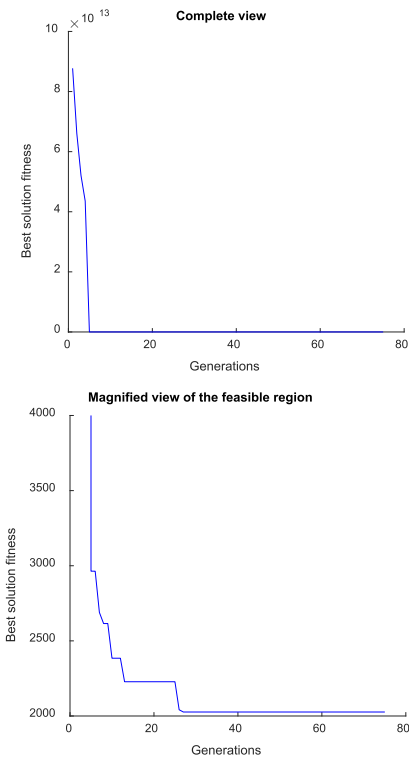
In this subsection, the case of fixed platforms for arrivals and departures of the same service type is considered. In the operation defined in this case study, trains performing a service type arrive at the platform assigned to the departures of the same service type.

In Table 3, the parameters of the genetic algorithm used to solve the upper level are shown. The model is implemented in MATLAB and the lower level is solved by means of the “linprog” function. The value of the constant b to calculate the fitness (Equation (21)) is set to 10^{11} to distinguish between feasible and non-feasible solutions.

The fitness (or, in other words, the time period W plus the penalty for non-feasible solutions) evolution of the best solution found at each generation is depicted in Figure 10. On the upper side of the figure, a complete view of the fitness evolution is represented. The value set for the constant b

TABLE 3. Upper level genetic algorithm parameters.

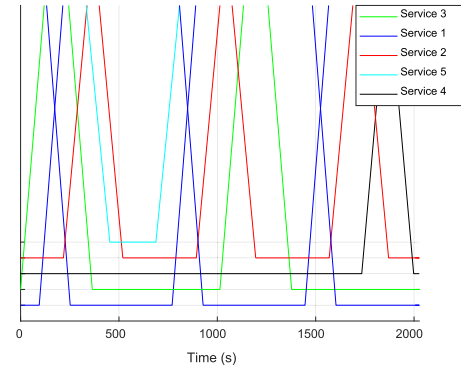
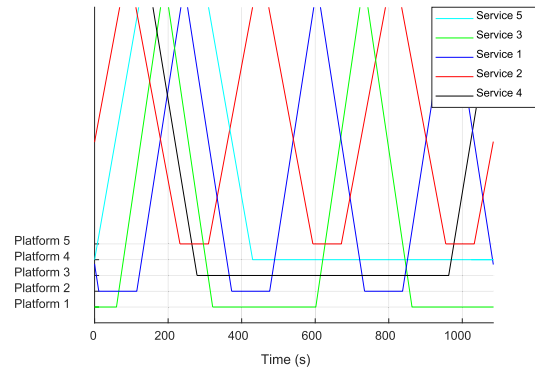
Population size (NP)	Number of survivors (NE)	Number of mutations (NM)	Number of crossovers (NC)	Number of generations (G)
40	8	20	10	75

**FIGURE 10.** Fitness evolution of the best solution found at each generation for the fixed platforms for arrivals and departures of the same service type case.

allows to graphically distinguish between unfeasible solutions (with fitness values on the order of 10¹³) and feasible solutions (with fitness values on the order of 10³). Thus, it can be seen that the algorithm starts evaluating unfeasible solutions up to generation 5. From this point, the best solution found by the algorithm is feasible. On the lower side of the figure, a magnified view of the fitness evolution in the feasible area is shown. From generation 5, the algorithm finds feasible solutions and starts to improve the time length for the period in the timetable of the solutions found. From generation 27, the result is stabilized in a solution with a period in the timetable of 2026 s.

In Figure 11, the timetable of the best solution obtained is graphically represented. As can be seen, all the services of the same type have regular departures and arrivals, maintaining a constant headway. Services of types 1, 2, 3, 4 and 5 are assigned to platforms 1, 4, 2, 3 and 5, respectively.

The solution derived from the proposed method effectively maximizes practical transport capacity. Importantly,

**FIGURE 11.** Timetable of the best solution for fuzzy practical transport capacity for the fixed platforms for arrivals and departures of the same service type case.**FIGURE 12.** Timetable of the best solution for crisp practical transport capacity for the fixed platforms for arrivals and departures of the same service type case.

the generated timetable accounts for operational robustness by modeling the arrival and departure times as fuzzy numbers. This solution can be compared with the crisp case, where the departure and arrival times are crisp numbers, to evaluate the increase in the time length of the timetable period. The crisp solution can be obtained using the same model but with a possibility of observing the minimum interval ($\Pi(\hat{t}_{diff} \geq I_{min})$) equal to 1 and a necessity of observing the minimum interval ($N(\hat{t}_{diff} \geq I_{min}) = 1 - \Pi(\hat{t}_{diff} < I_{min})$) equal to 0.

Figure 12 presents the timetable for the best solution found for the crisp case. In this timetable, the services of the same time maintain a constant headway as in the fuzzy case, but the period's time length is 1084 s. That means that the crisp timetable increases the transport capacity by 46%. However, this timetable has no time margins with respect to the minimum time interval between maneuvers. Thus, if a train is delayed, the subsequent trains will be delayed as well, and the planned operation cannot be recovered anymore. Therefore, the railway planner has to adjust the necessity of punctuality requirement considering the trade-off between the transport capacity and the timetable robustness.

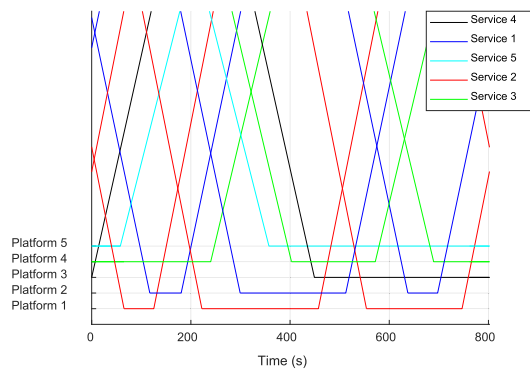


FIGURE 13. Timetable of the best solution for theoretical transport capacity for the fixed platforms for arrivals and departures of the same service type case.

An additional comparison can be made between the previous solutions and the maximum theoretical transport capacity solution. This second solution can be obtained by means of a crisp model with no restrictions related to the homogeneous headway between services of the same type. That means that the proposed model can be applied to obtain the maximum theoretical capacity with the previous requirements of necessity and possibility, and without restrictions formulated in (19) and (20).

The timetable for the maximum theoretical transport capacity is represented in Figure 13. As can be seen, the headway between services is not constant, as happened in previous cases. The length of the timetable period obtained for this case is 802 s. This value of transport capacity is 26% higher than the maximum crisp practical capacity solution. The variation between the maximum theoretical and practical capacity solutions highlights the importance of taking into account the operational rules with which the station will be exploited when assessing the transport capacity. Compared with the maximum fuzzy practical capacity, the difference is 60% in the length of the timetable period. This difference accounts not only for the constant headways' restriction but also for the robustness against delays. As can be seen, the value of theoretical transport capacity is far from achievable transport capacity, given that, in the theoretical case, the service provided to the passengers will be poor in terms of service regularity and punctuality.

D. STATION PRACTICAL CAPACITY EVALUATION FOR FIXED PLATFORMS FOR DEPARTURES OF THE SAME SERVICE TYPE AND FLEXIBLE ARRIVALS

In this subsection, the case of fixed platforms for departures of the same service type and flexible arrivals is considered. In the operation defined in this case study, trains performing a service type have to depart from the platform assigned, but arriving trains may be assigned to any platform regardless of their service type.

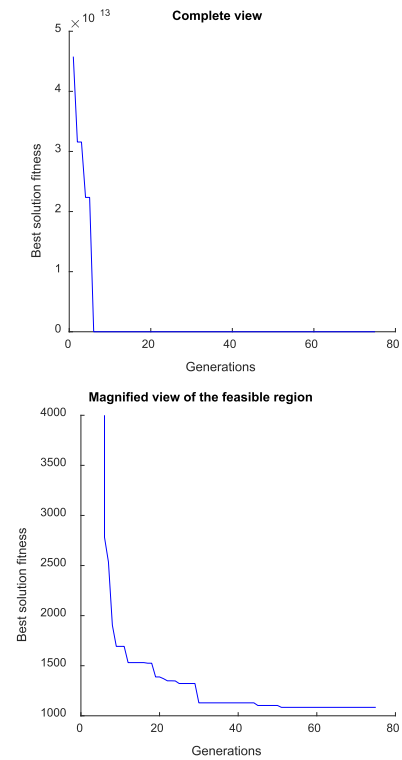


FIGURE 14. Fitness evolution of the best solution found at each generation for the fixed platforms for departures of the same service type and flexible arrivals case.

The same values for the fuzzy parameters and genetic algorithm configuration used in Section VII-C are applied in this case study.

The fitness evolution of the best solution found at each generation of the fuzzy maximum practical capacity model is depicted in Figure 14. On the upper side of the figure, a complete view of the fitness evolution is represented. As shown in the figure, the algorithm starts evaluating unfeasible solutions up to generation 6. From this point, the best solution found by the algorithm is feasible. On the lower side of the figure, a magnified view of the fitness evolution in the feasible area is shown. From generation 6, the algorithm finds feasible solutions and starts to improve the time length for the period in the timetable of the solutions found. From generation 51, the result is stabilized in a solution with a period in the timetable of 1085 s.

In Figure 15, the timetable of the best solution obtained is graphically represented. As can be seen, all the services of the same type have regular departures and arrivals, maintaining a constant headway. Departure of services of types 1, 2, 3, 4 and 5 are assigned to platforms 5, 1, 2, 3 and 4, respectively.

The results obtained represent an improvement of 46% in transport capacity compared to the operation analyzed in Section VII-C. Allowing a flexible arrival platform allows the algorithm to find a better coordination among arrival and departure routes, which translates to a more efficient station operation. This improvement in efficiency can be observed

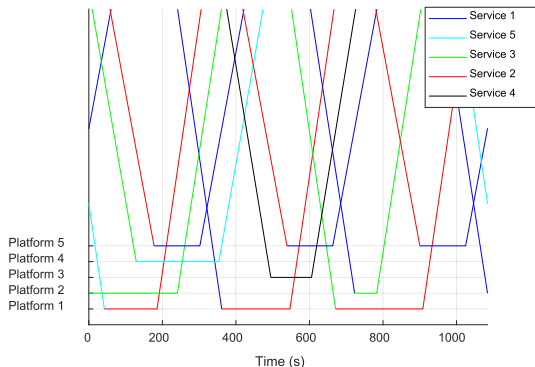


FIGURE 15. Timetable of the best solution for fuzzy practical transport capacity for the fixed platforms for departures of the same service type and flexible arrivals case.

by comparing the resulting timetables, as train dwell times are significantly reduced.

With this operational scheme, passengers can easily find their trains, as departures always take place from the same platforms. On the other hand, only arriving passengers who need to make a connection are affected, as they must orient themselves upon arrival to locate the platform for their next train. However, in this case study, it is required that both drivers and rolling stock be capable of performing any service type.

VIII. CONCLUSION

This paper presents a two-level optimization model for calculating the timetable and the platform assignment that maximizes the practical transport capacity of mass transit railway stations, a critical aspect of sustainable urban mobility. The proposed model integrates a genetic algorithm at the upper level to optimize the traffic pattern (train sequencing) and the platform assignment, while a linear programming model at the lower level optimizes the arrival/departure hour of each service to maximize the transport capacity.

Practical capacity is achieved by means of introducing the rules with which the station is exploited. In urban railways, typically, services of the same type (with the same arrival and destination) are operated, maintaining a constant headway between them. Thus, restrictions are introduced in the model's lower level to ensure that a uniform headway between services is obtained for each traffic pattern. The model allows the evaluation of two different operational scenarios: operation with fixed platforms for arrivals and departures of the same service type, and operation with fixed platforms for departures of the same service type with flexible arrivals. Moreover, fuzzy parameters are employed to incorporate operational uncertainties, ensuring a more robust and realistic capacity assessment. The inclusion of a detailed train simulation component further refines the accuracy of interval estimations, leading to improved reliability in the scheduling of train movements.

In this paper, it is shown that constant headway restrictions cause that many traffic patterns are not feasible. Therefore, a constraint handling method is introduced in the genetic algorithm at the upper level to guide the algorithm's search to feasible regions in the solution domain.

The application of the model to a real-world case study demonstrates its effectiveness in optimizing transport capacity in a mass transit railway station while maintaining operational feasibility. Results indicate that the fuzzy approach produces a realistic maximum transport capacity solution. Comparisons between theoretical transport capacity and fuzzy practical capacity highlight the trade-off between maximizing capacity and maintaining service robustness and regularity. The results obtained by the proposed model show that the regularity of the services is guaranteed by introducing the constant headway restriction, although a 26% decrease in transport capacity is observed compared with the theoretical one. An additional 34% of transport capacity decrease is obtained while introducing robustness in the timetable with a necessity of punctuality value equal to 0.5. Consequently, these results indicate that the theoretical transport capacity assessment is not realistic when evaluating a mass transit railway station because the solutions obtained are not applicable in real lines.

On the other hand, a significant improvement in transport capacity can be obtained by means of the operational scheme with fixed platforms for departures of the same service type and flexible arrivals (46%). However, this operation requires that both the rolling stock and train drivers can perform all types of services.

Future work will focus on extending the current optimization model to analyze not only individual stations but also the entire network of a mass transit system, incorporating additional constraints related to transfers between lines and with external transport modes. In addition, future work will consider expanding the terminal station topology to incorporate the possibility of platform-changing maneuvers behind the station (i.e., yard operations). In such cases, arrival and departure platforms do not need to be the same. If the station topology allows for these types of maneuvers, overall station capacity could be improved.

REFERENCES

- [1] P. Jovanović, N. Pavlović, I. Belošević, and S. Milinković, "Graph coloring-based approach for railway station design analysis and capacity determination," *Eur. J. Oper. Res.*, vol. 287, no. 1, pp. 348–360, Nov. 2020.
- [2] N. Weik and N. Nießen, "Quantifying the effects of running time variability on the capacity of rail corridors," *J. Rail Transp. Planning Manage.*, vol. 15, Sep. 2020, Art. no. 100203, doi: [10.1016/j.rtpm.2020.100203](https://doi.org/10.1016/j.rtpm.2020.100203).
- [3] M. Mikulčić and T. J. Mlinarić, "Railway capacity enhancement with modern signalling systems – a literature review," *Promet-Traffic Transp.*, vol. 33, no. 1, pp. 141–152, Feb. 2021, doi: [10.7307/ptt.v33i1.3664](https://doi.org/10.7307/ptt.v33i1.3664).
- [4] X. Jia, R. He, and H. Chai, "Optimizing the number of express freight trains on a high-speed railway corridor by the departure period," *IEEE Access*, vol. 8, pp. 100058–100072, 2020, doi: [10.1109/ACCESS.2020.2995176](https://doi.org/10.1109/ACCESS.2020.2995176).
- [5] *FUTURAIL. Next-Gen Urban Railway Transport: Smart Planning and Regulation for Capacity and Energy Efficiency*, MICIU/AEI/10.13039/501100011033, NextGenerationEU/PRTR, Spain, 2025.

[6] F. Zhou, X. Song, R. Xu, and C. Ji, "Optimization of urban rail transit connection scheme for evacuating large volumes of arriving railway passengers," *IEEE Access*, vol. 8, pp. 68772–68786, 2020, doi: [10.1109/ACCESS.2020.2985863](https://doi.org/10.1109/ACCESS.2020.2985863).

[7] *UIC Code 406: Capacity*, Int. Union Railways, Paris, France, 2013.

[8] M. Abril, F. Barber, L. Ingolotti, M. A. Salido, P. Tormos, and A. Lova, "An assessment of railway capacity," *Transp. Res. E, Logistics Transp. Rev.*, vol. 44, no. 5, pp. 774–806, Sep. 2008, doi: [10.1016/j.tre.2007.04.001](https://doi.org/10.1016/j.tre.2007.04.001).

[9] M. Khadem Sameni and A. Moradi, "Railway capacity: A review of analysis methods," *J. Rail Transp. Planning Manage.*, vol. 24, Dec. 2022, Art. no. 100357, doi: [10.1016/j.jrtpm.2022.100357](https://doi.org/10.1016/j.jrtpm.2022.100357).

[10] *UIC Code 406: Capacity*, Int. Union Railways, Paris, France," 2004.

[11] T. Lindner, "Applicability of the analytical UIC code 406 compression method for evaluating line and station capacity," *J. Rail Transp. Planning Manage.*, vol. 1, no. 1, pp. 49–57, Nov. 2011, doi: [10.1016/j.jrtpm.2011.09.002](https://doi.org/10.1016/j.jrtpm.2011.09.002).

[12] A. Kavička, R. Diviš, and P. Veselý, "Railway station capacity assessment utilizing simulation-based techniques and the UIC406 method," in *Proc. 32nd Eur. Modeling Simulation Symp. (EMSS)*, 2020, pp. 41–49.

[13] I. Johansson and N. Weik, "Strategic assessment of railway station capacity-urther development of a UIC 406-based approach considering timetable uncertainty," presented at the 9th Int. Conf. Railway Oper. Modelling Anal. (ICROMA), Beijing, China, Jun. 2021, pp. 3–7. [Online]. Available: <https://urn.kb.se/resolve?urn=urn:nbn:se:kth:diva-306071>

[14] Q. Zhong, C. Xu, R. Yang, and Q. Zhong, "Equivalences between analytical railway capacity methods," *J. Rail Transp. Planning Manage.*, vol. 25, Mar. 2023, Art. no. 100367, doi: [10.1016/j.jrtpm.2022.100367](https://doi.org/10.1016/j.jrtpm.2022.100367).

[15] R. Francesco, M. Gabriele, and R. Stefano, "Complex railway systems: Capacity and utilisation of interconnected networks," *Eur. Transp. Res. Rev.*, vol. 8, no. 4, p. 29, Nov. 2016, doi: [10.1007/s12544-016-0216-6](https://doi.org/10.1007/s12544-016-0216-6).

[16] L. Valentinić and H. Sivilevicius, "Railway line capacity methods analysis and their application in 'Lithuanian railways' justification," in *Proc. Int. Conf. Environ. Eng.*, 2014, p. 1.

[17] G. Malavasi, T. Molková, S. Ricci, and F. Rotoli, "A synthetic approach to the evaluation of the carrying capacity of complex railway nodes," *J. Rail Transp. Planning Manage.*, vol. 4, nos. 1–2, pp. 28–42, Aug. 2014.

[18] J. Wang, Y. Yu, R. Kang, and J. Wang, "A novel space-time-speed method for increasing the passing capacity with safety guaranteed of railway station," *J. Adv. Transp.*, vol. 2017, pp. 1–11, 2017, doi: [10.1155/2017/6381718](https://doi.org/10.1155/2017/6381718).

[19] J. Armstrong and J. Preston, "Capacity utilisation and performance at railway stations," *J. Rail Transp. Planning Manage.*, vol. 7, no. 3, pp. 187–205, Dec. 2017, doi: [10.1016/j.jrtpm.2017.08.003](https://doi.org/10.1016/j.jrtpm.2017.08.003).

[20] J. Yuan and I. A. Hansen, "Optimizing capacity utilization of stations by estimating knock-on train delays," *Transp. Res. B, Methodol.*, vol. 41, no. 2, pp. 202–217, Feb. 2007.

[21] L. Yang, L. Zhou, H. Zhou, C. Han, and W. Zhao, "A Lagrangian method for calculation of passing capacity on a railway hub station," *Mathematics*, vol. 11, no. 6, p. 1418, Mar. 2023, doi: [10.3390/math11061418](https://doi.org/10.3390/math11061418).

[22] J. Lordieck, M. Nold, and F. Cormann, "Microscopic railway capacity assessment of heterogeneous traffic under real-life operational conditions," *J. Rail Transp. Planning Manage.*, vol. 30, Jun. 2024, Art. no. 100446, doi: [10.1016/j.jrtpm.2024.100446](https://doi.org/10.1016/j.jrtpm.2024.100446).

[23] L. W. Jensen, A. Landex, O. A. Nielsen, L. G. Kroon, and M. Schmidt, "Strategic assessment of capacity consumption in railway networks: Framework and model," *Transp. Res. C, Emerg. Technol.*, vol. 74, pp. 126–149, Jan. 2017.

[24] T. Emunds and N. Nießen, "Evaluating railway junction infrastructure: A queueing-based, timetable-independent analysis," *Transp. Res. C, Emerg. Technol.*, vol. 165, Aug. 2024, Art. no. 104704, doi: [10.1016/j.trc.2024.104704](https://doi.org/10.1016/j.trc.2024.104704).

[25] C. Szymula, N. Bešinović, and K. Nachtigall, "Quantifying periodic railway network capacity using Petri nets and macroscopic fundamental diagram," *Transp. Res. C, Emerg. Technol.*, vol. 158, Jan. 2024, Art. no. 104436, doi: [10.1016/j.trc.2023.104436](https://doi.org/10.1016/j.trc.2023.104436).

[26] C. Szymula, N. Bešinović, and K. Nachtigall, "Demand-based capacity assessment using mixed integer programming," *J. Rail Transp. Planning Manage.*, vol. 33, Mar. 2025, Art. no. 100502, doi: [10.1016/j.jrtpm.2024.100502](https://doi.org/10.1016/j.jrtpm.2024.100502).

[27] H. Pouryousef and P. Lautala, "Hybrid simulation approach for improving railway capacity and train schedules," *J. Rail Transp. Planning Manage.*, vol. 5, no. 4, pp. 211–224, Dec. 2015.

[28] A. Dicembre and S. Ricci, "Railway traffic on high density urban corridors: Capacity, signalling and timetable," *J. Rail Transp. Planning Manage.*, vol. 1, no. 2, pp. 59–68, Dec. 2011.

[29] I. Ljubaj and T. J. Mlinarić, "The possibility of utilising maximum capacity of the double-track railway by using innovative traffic organisation," *Transp. Res. Proc.*, vol. 40, pp. 346–353, Jan. 2019.

[30] L. M. Navarro, A. Fernandez-Cardador, and A. P. Cucala, "Fuzzy maximum capacity and occupancy time rate measurements in urban railway lines," *Eur. Transp. Res. Rev.*, vol. 10, no. 2, p. 61, Dec. 2018, doi: [10.1186/s12544-018-0335-3](https://doi.org/10.1186/s12544-018-0335-3).

[31] M. H. Dingler, Y.-C.-Lai, and C. P. L. Barkan, "Impact of train type heterogeneity on single-track railway capacity," *Transp. Res. Rec.*, vol. 2117, no. 1, pp. 41–49, Jan. 2009, doi: [10.3141/2117-06](https://doi.org/10.3141/2117-06).

[32] Y.-C.-Lai, Y.-H. Liu, and T.-Y. Lin, "Development of base train equivalents to standardize trains for capacity analysis," *Transp. Res. Rec.*, vol. 2289, no. 1, pp. 119–125, Jan. 2012.

[33] M. H. Dingler, Y.-C. R. Lai, and C. P. Barkan, "Effect of train-type heterogeneity on single-track heavy haul railway line capacity," *Proc. Inst. Mech. Eng., F, J. Rail Rapid Transit*, vol. 228, no. 8, pp. 845–856, Nov. 2014, doi: [10.1177/0954409713496762](https://doi.org/10.1177/0954409713496762).

[34] Y.-C. Lai, Y.-A. Huang, and H.-Y. Chu, "Estimation of rail capacity using regression and neural network," *Neural Comput. Appl.*, vol. 25, nos. 7–8, pp. 2067–2077, Dec. 2014, doi: [10.1007/s00521-014-1694-x](https://doi.org/10.1007/s00521-014-1694-x).

[35] T.-Y. Lin, Y.-C. Lin, and Y.-C. R. Lai, "Base train equivalents for multiple train types based delay-based capacity analysis," *J. Transp. Eng., A, Syst.*, vol. 146, no. 5, May 2020, Art. no. 04020023, doi: [10.1061/jtepbs.0000039](https://doi.org/10.1061/jtepbs.0000039).

[36] R. M. P. Goverde, F. Cormann, and A. D'Ariano, "Railway line capacity consumption of different railway signalling systems under scheduled and disturbed conditions," *J. Rail Transp. Planning Manage.*, vol. 3, no. 3, pp. 78–94, Aug. 2013, doi: [10.1016/j.jrtpm.2013.12.001](https://doi.org/10.1016/j.jrtpm.2013.12.001).

[37] K. M. Kim, S.-M. Oh, S.-J. Ko, and B. H. Park, "New headway-based analytical capacity model considering heterogeneous train traffic," *J. Transp. Eng., A, Syst.*, vol. 146, no. 12, Dec. 2020, Art. no. 04020135, doi: [10.1061/jtepbs.0000461](https://doi.org/10.1061/jtepbs.0000461).

[38] S. Han, Y. Yue, and L. Zhou, "Carrying capacity of railway station by microscopic simulation method," in *Proc. 17th Int. IEEE Conf. Intell. Transp. Syst. (ITSC)*, Oct. 2014, pp. 2725–2731, doi: [10.1109/ITSC.2014.6958126](https://doi.org/10.1109/ITSC.2014.6958126).

[39] M. Zhong, Y. Yue, and D. Li, "Analyzing and evaluating infrastructure capacity of railway passenger station by mesoscopic simulation method," in *Proc. Int. Conf. Intell. Rail Transp. (ICIRT)*, Dec. 2018, pp. 1–5, doi: [10.1109/ICIRT.2018.8641593](https://doi.org/10.1109/ICIRT.2018.8641593).

[40] J. Bulíček, P. Nachtigall, J. Široký, and E. Tischer, "Improving single-track railway line capacity using extended station switch point area," *J. Rail Transp. Planning Manage.*, vol. 24, Dec. 2022, Art. no. 100354.

[41] P. Veselý, A. Kavicka, and P. Krýze, "Automated construction of mesoscopic railway infrastructure models supporting station throat capacity assessment," *IEEE Access*, vol. 11, pp. 37869–37899, 2023, doi: [10.1109/ACCESS.2023.3266813](https://doi.org/10.1109/ACCESS.2023.3266813).

[42] D. Knutsen, N. O. E. Olsson, and J. Fu, "Capacity evaluation of ERTMS/ETCS hybrid level 3 using simulation methods," *J. Rail Transp. Planning Manage.*, vol. 30, Jun. 2024, Art. no. 100444, doi: [10.1016/j.jrtpm.2024.100444](https://doi.org/10.1016/j.jrtpm.2024.100444).

[43] P. Sels, B. Waquet, T. Dewilde, D. Catrysse, and P. Vansteenwegen, "Calculation of realistic railway station capacity by platforming feasibility checks," in *Proc. 2nd Int. Conf. Models Technol. ITS*, Jun. 2011, pp. 1–4.

[44] N. Javadian, H. R. Sayarshad, and S. Najafi, "Using simulated annealing for determination of the capacity of yard stations in a railway industry," *Appl. Soft Comput.*, vol. 11, no. 2, pp. 1899–1907, Mar. 2011.

[45] M. Yaghini, N. Nikoo, and H. R. Ahadi, "An integer programming model for analysing impacts of different train types on railway line capacity," *Transport*, vol. 29, no. 1, pp. 28–35, Mar. 2014, doi: [10.3846/16484142.2014.894938](https://doi.org/10.3846/16484142.2014.894938).

[46] M. Khadem Sameni, J. Preston, and M. Khadem Sameni, "Evaluating efficiency of passenger railway stations: A DEA approach," *Res. Transp. Bus. Manage.*, vol. 20, pp. 33–38, Sep. 2016.

[47] R. L. Burdett, "Multi-objective models and techniques for analysing the absolute capacity of railway networks," *Eur. J. Oper. Res.*, vol. 245, no. 2, pp. 489–505, Sep. 2015.

[48] L. W. Jensen, "An optimisation framework for determination of capacity in railway networks," in *Proc. 13th Conf. Adv. Syst. Public Transp.*, Jan. 2015.

[49] B. Guo, L. Zhou, Y. Yue, and J. Tang, "A study on the practical carrying capacity of large high-speed railway stations considering train set utilization," *Math. Problems Eng.*, vol. 2016, pp. 1–11, Jan. 2016, doi: [10.1155/2016/2741479](https://doi.org/10.1155/2016/2741479).

[50] T. Dollevoet, D. Huisman, L. Kroon, M. Schmidt, and A. Schöbel, "Delay management including capacities of stations," *Transp. Sci.*, vol. 49, no. 2, pp. 185–203, May 2015, doi: [10.1287/trsc.2013.0506](https://doi.org/10.1287/trsc.2013.0506).

[51] J. Wu and C. Zhang, "Research on calculation method of passing capacity of high speed railway station and design of simulation process," *Dept. Elect. Eng. and Comput. Sci., Inst. Electron. Comput., Tech. Rep.*, 2019, pp. 39–44, vol. 1, doi: [10.33969/EECS.V1.006](https://doi.org/10.33969/EECS.V1.006).

[52] A. N. Ignatov and A. V. Naumov, "On the problem of increasing the railway station capacity," *Autom. Remote Control*, vol. 82, no. 1, pp. 102–114, Jan. 2021, doi: [10.1134/s0005117921010070](https://doi.org/10.1134/s0005117921010070).

[53] Z. Liao and C. Mu, "Assessing the compatibility of railway station layouts and mixed heterogeneous traffic patterns by optimization-based capacity estimation," *Mathematics*, vol. 11, no. 17, p. 3727, Aug. 2023, doi: [10.3390/math11173727](https://doi.org/10.3390/math11173727).

[54] R. E. Bellman and L. A. Zadeh, "Decision-making in a fuzzy environment," *Manage. Sci.*, vol. 17, no. 4, pp. B-141–B-164, Dec. 1970, doi: [10.1287/mnsc.17.4.b141](https://doi.org/10.1287/mnsc.17.4.b141).

[55] L. Wang, Y. Qin, J. Xu, and L. Jia, "A fuzzy optimization model for high-speed railway timetable rescheduling," *Discrete Dyn. Nature Soc.*, vol. 2012, no. 1, Dec. 2012, doi: [10.1155/2012/827073](https://doi.org/10.1155/2012/827073).

[56] Y. V. Bocharnikov, A. M. Tobias, C. Roberts, S. Hillmansen, and C. J. Goodman, "Optimal driving strategy for traction energy saving on DC suburban railways," *IET Electr. Power Appl.*, vol. 1, no. 5, pp. 675–682, Sep. 2007, doi: [10.1049/iet-epa:20070005](https://doi.org/10.1049/iet-epa:20070005).

[57] L. Yang, K. Li, and Z. Gao, "Train timetable problem on a single-line railway with fuzzy passenger demand," *IEEE Trans. Fuzzy Syst.*, vol. 17, no. 3, pp. 617–629, Jun. 2009, doi: [10.1109/TFUZZ.2008.924198](https://doi.org/10.1109/TFUZZ.2008.924198).

[58] A. P. Cucala, A. Fernández, C. Sicre, and M. Domínguez, "Fuzzy optimal schedule of high speed train operation to minimize energy consumption with uncertain delays and driver's behavioral response," *Eng. Appl. Artif. Intell.*, vol. 25, no. 8, pp. 1548–1557, Dec. 2012, doi: [10.1016/j.engappai.2012.02.006](https://doi.org/10.1016/j.engappai.2012.02.006).

[59] W. Carvajal-Carreño, A. P. Cucala, and A. Fernández-Cardador, "Optimal design of energy-efficient ATO CBTC driving for metro lines based on NSGA-II with fuzzy parameters," *Eng. Appl. Artif. Intell.*, vol. 36, pp. 164–177, Nov. 2014, doi: [10.1016/j.engappai.2014.07.019](https://doi.org/10.1016/j.engappai.2014.07.019).

[60] C. Sicre, A. P. Cucala, and A. Fernández-Cardador, "Real time regulation of efficient driving of high speed trains based on a genetic algorithm and a fuzzy model of manual driving," *Eng. Appl. Artif. Intell.*, vol. 29, pp. 79–92, Mar. 2014, doi: [10.1016/j.engappai.2013.07.015](https://doi.org/10.1016/j.engappai.2013.07.015).

[61] A. Fernández-Rodríguez, A. Fernández-Cardador, and A. P. Cucala, "Balancing energy consumption and risk of delay in high speed trains: A three-objective real-time eco-driving algorithm with fuzzy parameters," *Transp. Res. C, Emerg. Technol.*, vol. 95, pp. 652–678, Oct. 2018, doi: [10.1016/j.trc.2018.08.009](https://doi.org/10.1016/j.trc.2018.08.009).

[62] Z. Xiao, S. Xia, K. Gong, and D. Li, "The trapezoidal fuzzy soft set and its application in MCDM," *Appl. Math. Model.*, vol. 36, no. 12, pp. 5844–5855, Dec. 2012, doi: [10.1016/j.apm.2012.01.036](https://doi.org/10.1016/j.apm.2012.01.036).

[63] P. Vasant, T. Ganesan, and I. Elamvazuthi, "Improved Tabu search recursive fuzzy method for crude oil industry," *Int. J. Model. Simul. Sci. Comput.*, vol. 3, no. 1, Mar. 2012, Art. no. 1150002, doi: [10.1142/s1793962311500024](https://doi.org/10.1142/s1793962311500024).

[64] Chan, "An approximation approach for representing S-Shaped membership functions," *IEEE Trans. Fuzzy Syst.*, vol. 18, no. 2, pp. 412–424, Apr. 2010, doi: [10.1109/TFUZZ.2010.2042961](https://doi.org/10.1109/TFUZZ.2010.2042961).

[65] T. Baeck, D. B. Fogel, and Z. Michalewicz, *Handbook of Evolutionary Computation*. Boca Raton, FL, USA: CRC Press, 1997, doi: [10.1201/9781420050387](https://doi.org/10.1201/9781420050387).

[66] D. Dubois and H. Prade, "Ranking fuzzy numbers in the setting of possibility theory," *Inf. Sci.*, vol. 30, no. 3, pp. 183–224, Sep. 1983, doi: [10.1016/0020-0255\(83\)90025-7](https://doi.org/10.1016/0020-0255(83)90025-7).

[67] S. Chanas, W. Kołodziejczyk, and A. Machaj, "A fuzzy approach to the transportation problem," *Fuzzy Sets Syst.*, vol. 13, no. 3, pp. 211–221, Aug. 1984, doi: [10.1016/0165-0114\(84\)90057-5](https://doi.org/10.1016/0165-0114(84)90057-5).

[68] A. Fernández-Rodríguez, A. Fernández-Cardador, and A. P. Cucala, "Real time eco-driving of high speed trains by simulation-based dynamic multi-objective optimization," *Simul. Model. Pract. Theory*, vol. 84, pp. 50–68, May 2018, doi: [10.1016/j.simpat.2018.01.006](https://doi.org/10.1016/j.simpat.2018.01.006).

[69] *ERTMS/ETCS-System Requirements Specification*, ERA, Valenciennes, France, 2016.



ADRIÁN FERNÁNDEZ-RODRÍGUEZ received the industrial engineering degree from the Universidad Politécnica de Madrid, in 2012, and the Ph.D. degree from Comillas Pontifical University, Madrid, in 2018.

He is currently a Research Fellow with the Railway Research Group of Institute for Research in Technology, Comillas Pontifical University. His research interests include train operation modeling, energy efficiency in railways, and nature inspired optimization.



MARÍA DOMÍNGUEZ received the industrial engineering and Ph.D. degrees from Comillas Pontifical University, Madrid, Spain.

She is currently a Research Fellow with the Railway Research Group of Institute for Research in Technology, Comillas Pontifical University. Her research interests include train simulation, eco-driving, and energy efficiency in railways.



ASUNCIÓN P. CUCALA received the industrial engineering and Ph.D. degrees from Comillas Pontifical University, Madrid, Spain.

She is currently the Director of the Institute for Research in Technology, a Research Fellow of the Railways Research Group, and a Full Professor with the ICAI School of Engineering, Comillas Pontifical University. Her research interests include train simulation, railways operation and control, energy efficiency in railways, and railway capacity analysis.



ANTONIO FERNÁNDEZ-CARDADOR received the degree in physics from the Universidad Complutense de Madrid, Spain, and the Ph.D. degree from Comillas Pontifical University, Madrid.

He is currently a Research Fellow with the Railways Research Group, Institute for Research in Technology, and a Full Professor with the ICAI School of Engineering, Comillas Pontifical University. His research interests include train simulation, railways operation and control, eco-driving, and railway capacity.